CNMAC2012
XXXIV CONGRESSO NACIONAL DE
MATEMÁTICA APLICADA E COMPUTACIONAL
17 a 21 de setembro de 2012 – Águas de Lindóia/SP

ISSN 1984-8218

How heterogeneity increases the range of bursting in a small network of pre-Bötzinger complex cells

Evandro Manica,
Depto de Matemática, UFRGS,
90650-000, Porto Alegre, RS
E-mail: evandro.manica@ufrgs.br,

Jonathan Rubin
Department of Mathematics - University of Pittsburgh
15260, Pittsburgh, PA, USA
E-mail: rubin@math.pitt.edu.

Abstract: *In this work we run some simulations to show how heterogeneity can increase the range of bursting in a small network of neurons of the pre-Bötzinger complex (pre-BötC).*

Keywords: *pre-BötC, heterogenity, breathing*

1 Introduction

Breathing is a deceptively simple yet remarkable behavior in vertebrates [7]. It is one of the most vital processes of our bodies, occurring continuously and automatically from the time we are born until the day we die.

The *pre-Bötzinger complex* (preBötC) is a site in the ventrolateral medula which is believed to play an important role for controlling the respiratory rhythm in mammals, especially the inspiration process [9]. The importance of the preBötC is supported by experiments *in vivo* and *in vitro*, in rats, showing that any damage to the preBötC causes disturbances in the inspiratory phase of breathing. Diseases which attack the neurosystem responsible for breathing, in humans, include: Parkinson's disease, multiple syndrome atrophy and amyotrophic lateral sclerosis [2, 1].

As observed in experiments *in vitro*, during inhalation, cells in the preBötC are in their *active phase* and during exhalation, cells go *silent*. These alternating phases of activity and silence form a rhythm called *bursting*. During each active phase, cells experience two or more abrupt changes in the membrane potential (that is, the difference in charge across a cell's membrane) followed by a period of recovery (where we do not see any activity) . Each of these abrupt changes is called a *spike*.

The inspiration process is connected to synchronized oscillatory bursting behavior of the preBötC cells. Butera *et al* [4, 5] develop a nonlinear differential equation model network of cells based on the *Hodgkin and Huxley* formalism [8] exhibiting synchronized bursting activity consistent with that observed experimentally in respiration. Simulations show that some of the mechanisms that confer such adaptability are *coupling* and *heterogeneity*, complying with experiments *in vitro*.

Best *et al* [3] explores a network of a single self-coupled cell and a model network with two coupled identical cells from the preBötC, based on the Butera model. In their work, they found regions for some key parameters, namely g_{syn} and g_{ton}, where the cells are either silent, bursting or continuously spiking (tonically active). In an experiment, these quantities can be changed and can affect the dynamic behavior of the network.

ISSN 1984-8218

The role of heterogeneity and coupling in the *pre-BötC*, is studied by means of simulations of a minimal two cell network to isolate key mechanisms of the full system. Although, numerically we can see how heterogeneity and coupling change the behavior of the network, the specific mechanisms through which these effects occur remain to be understood. Using fast/slow decomposition and bifurcation analysis (same used in [3]), numerical analysis was performed by perturbing slightly the degree of heterogeneity of the sodium current, namely δ, across the two cells and analyzing the behavior of the network. In this heterogeneous context, each of the cells may be engaged in a different activity pattern. To the best of our knowledge, this type of behavior has not previously been analyzed in the study of small neural networks in the brainstem.

2 Model Equations

In this section, a sligth modification of the Butera's minimal model [4, 5] of a network of preBötC cells modeling the inspiratory phase of respiration. Butera's model followed the usual Hodgkin-Huxley formalism [8] using voltage-gated variables to account for the different behaviors. Butera's numerical results are consistent with what has been seen in experiments *in vitro* [4, 5].

The set of equations describing the dynamics of a small network of preBötC cells using voltage-gated variables is given by [3, 4, 5]

$$v_i' = \frac{-I_{NaP}(v_i) - I_{Na}(v_i, n_i) - I_K(v_i, n_i) - I_L(v_i) - I_{ton}(v_i) - I_{syn}(v_i)}{C} \quad (1)$$

$$h_i' = \epsilon \frac{h_\infty(v_i) - h_i}{\tau_h(v_i)} \quad (2)$$

$$n_i' = \frac{n_\infty(v_i) - n}{\tau_n(v_i)} \quad (3)$$

$$s_i' = \alpha_s(1 - s_i)s_\infty(v_j) - \frac{s_i}{\tau_s}, \quad (4)$$

where C is the capacitance of the cell ; v_i is the membrane potential of the cell; h_i and n_i are inactivation and activation variables, respectively; s_i is the synaptic coupling; τ_s is a positive time constant and ϵ is a small and positive constant. The right-hand side of (1) is the sum of all inward and outward currents and their expressions are given below:

$$\begin{aligned} I_{NaP}(v_i) &= \bar{g}_{NaP} m_{P,\infty}(v_i) h(v_i - E_{Na}), \quad I_{Na}(v_i) = \bar{g}_{Na} m_\infty(v_i)^3 (1 - n_i)(v_i - E_{Na}), \\ I_K(v_i) &= \bar{g}_K n_i^4 (v_i - E_K); \quad I_L(v_i) = \bar{g}_L(v_i - E_L), \\ I_{ton}(v_i) &= \bar{g}_{ton}(v_i - E_{syn}), \quad I_{syn}(v_i) = \bar{g}_{syn} s_i (v_i - E_{syn}). \end{aligned}$$

Above, E_{Na}, E_K, E_L and E_{syn} are resting potentials for the sodium, potassium, leakage and synaptic currents, respectively; $\bar{g}_{NaP}$, $\bar{g}_{Na}$, $\bar{g}_K$, $\bar{g}_L$, $\bar{g}_{ton}$ and $\bar{g}_{syn}$ are the maximal conductances for the persistent sodium, sodium, potassium, leakage, tonic and synaptic currents, respectively. Their values with respective units are given in table 1. Finally,

$$\begin{aligned} m_{P,\infty}(v_i) &= \frac{1}{1 + e^{\frac{v_i + 40}{-6}}}, \; n_\infty(v_i) = \frac{1}{1 + e^{\frac{v_i + 29}{-4}}}, \quad m_\infty(v_i) = \frac{1}{1 + e^{\frac{v_i + 34}{-5}}}, \quad h_\infty(v_i) = \frac{1}{1 + e^{\frac{v_i + 48}{6}}}, \\ s_\infty(v_i) &= \frac{1}{1 + e^{\frac{v_i + 10}{-5}}}, \quad \tau_h(v_i) = \frac{\bar{\tau}_h}{cosh\left(\frac{v_i + 48}{12}\right)}, \; \tau_n(v_i) = \frac{10}{cosh\left(\frac{v_i + 29}{-8}\right)}, \end{aligned}$$

for $i = 1, 2$, where $y_\infty(v_i)$ with $y \in \{m, n, h, s\}$ are steady-state voltage-dependent functions and $\tau_h(v_i)$ and $\tau_h(v_i)$ are voltage-dependent time constants. Also $\frac{\bar{\tau}_h}{\epsilon} = 10000 msec$. For more details about the connection with biological experiments, see for example [4].

ISSN 1984-8218

$\bar{g}_{NaP}$	$\bar{g}_{Na}$	E_{Na}	$\bar{g}_K$	E_K	$\bar{g}_L$	E_L	$\bar{g}_{ton}$	E_{syn}	$\bar{g}_{syn}$
2.8 nS	28 nS	50 mV	11.2 nS	-85 mV	2.8 nS	-65 mV	[0;1] nS	0 mV	[0;15] nS

Tabela 1: Values of some parameters as given in [3] with respective units

For the 2-cell coupled case, $i = 1, 2$ and $j = 3 - i$. In this model, bursting can be started and terminated through fast activation and slow inactivation of the I_{NaP} current. In this work, we used a slight different model by means of the change of variables $t = 10T$, $v = 100V$, and $\bar{g^\star}_i = \frac{\bar{g}_i}{g_{Na}}$ (maximal conductances) applied to the original set of equations (1)-(4).

3 Some Numerical Results

In this section, we show the effect of having g_{NaP} different for the two cells, say g_{NaP_1} and g_{NaP_2}. In the two cell case with the two cells with the same parameters, [3] determined all possible regimes and transitions on the (g_{syn}, g_{ton}) parameter space. Here for fixed g_{syn} and $\delta = 2.8 - g_{NaP_1} = g_{NaP_2} - 2.8$ with $\delta > 0$ and 2.8 the baseline value of g_{NaP} [4], we will see how the dynamics of the cell changes with (g_{ton}, δ) and we will compare our results to [3]. In this set up, δ measures the level of heterogeneity present in the network.

All the analysis done here includes computing the averaged nullclines

$$N_i(h_1, h_2) = \frac{1}{T_s(h_1, h_2)} \int_0^{T_s(h_1,h_2)} g_i(v_i) d\xi \qquad i = 1, 2, \tag{5}$$

where $g_i(v_i) \equiv \epsilon \frac{(h_\infty(v_i) - h_i)}{\tau_h(v_i)}$ and $T_s(h_1, h_2)$ is the period of the fast subsystem periodic orbit being averaged for each fixed (h_1, h_2) inside the oscillatory region O(active phase).

The goal here is to determine from the homogeneous case (studied by [3]) how the dynamic range of bursting is affected by heterogeneity in g_{NaP}. Based on the configuration of the nullclines, on whether the averaged nullclines intersect inside O and on the stability of any resulting fixed points inside the O, we will determine changes in the dynamical behavior for different g_{NaP}. Numerical results (not shown here) that an increase in δ implies that both averaged nullclines move to the right and down. The overall effect of increasing δ is to move the nullclines to larger values of h_1 and lower values of h_2.

3.1 Classifying dynamic regimes

In order to possibly determine boundaries for the transition between different regimes similar to the bellycurve in [3], we fixed g_{syn} and varied g_{ton} and δ.

3.1.1 Different regions of bursting and spiking for $g_{syn} = 3$

Before proceeding further, let us set up some notation and make some connections to the homogeneous case. In the homogeneous case, the averaged nullclines can intersect 1 or 3 times in O depending on the value of the parameters. Moreover, a pitchfork bifurcation of periodics occurs as the parameter g_{ton} is increased, due to the symmetry of the fixed points on the (h_1, h_2) plane. In the heterogeneous case, it is possible to have 1, 2 or 3 intersections of the nullclines inside O, and each possibility will lead to a different behavior. The fixed points will be defined as follows: f_p^0 denotes a fixed point near the line $h_1 = h_2$; f_p^1 denotes a fixed point for $h_1 > h_2$ and f_p^2 denotes a fixed point for $h_2 > h_1$.

In figure 1, a cartoon shows a generic result of symmetry breaking applied to a pitchfork bifurcation when different levels of heterogeneity are applied to this small network for $g_{syn} = 3$ and g_{ton} as a bifurcation parameter. Next, consider numerical results to assess the details of the transitions in the heterogeneous case.

ISSN 1984-8218

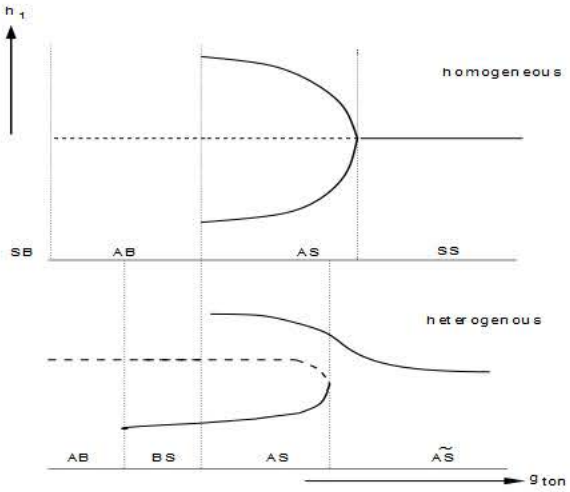

Figura 1: Cartoons representing pitchfork bifurcation for the cells in the homogeneous and heterogeneous cases.

In figure 2 (Left), we show numerically how varying g_{ton} and δ with $g_{syn} = 3$ affected the dynamics of the 2 cells. In this picture, $\delta = 0$ represents the homogeneous case and $g_{ton} = 0.856$ and $g_{ton} = 0.898$ represent the values for the transition from **AB** to **AS** and **AS** to **SS**, respectively. For $\delta > 0$, the transitions between different regimes were determined as follows. Fixing $\delta = 0.01$, we systematically varied g_{ton} from lower to higher values and for various initial conditions. If 2 consecutive values of g_{ton} were giving completely different results on the (V_1, t), (V_2, t) and (h_1, h_2) planes, then the boundary for the transition from one regime to another was determined.

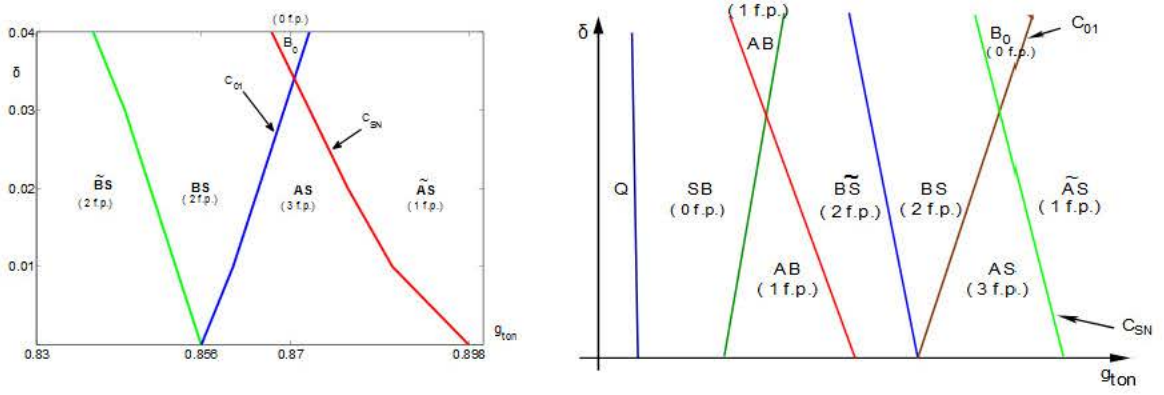

Figura 2: Left: Different types of bursting and spiking for $g_{syn} = 3$. C_{SN} is a curve of saddle node points and C_{01} indicates that a fixed point enters the oscillatory region. Right: Cartoon showing all possible different types of bursting and spiking for $g_{syn} = 3$.

In figure 2 (Right), a more complete description of the different regimes we expect to find for $g_{syn} = 3$, based on the numerical results presented on the figure 2 (Left) and numerical simulations for various g_{ton} and δ using XPP/AUTO [6].

Now, let's describe what each of the regions presented on figure 2 represent for increasing g_{ton}.

1. region **Q**: represents the values of g_{ton} and δ, on the (g_{ton}, δ) plane so that the two cells are silent. For $\delta \neq 0$, the boundary of **Q** (dark blue curve) moves slightly to the left indicating that the transition from quiescence to bursting will occur for a lower value of g_{ton} as we increase δ.

ISSN 1984-8218

2. region **SB**: Cells are bursting. For all initial conditions trajectories of the full system approach reasonably close to the identity line and deviate from the identity line at the end of the active phase (figure not shown). Average nullclines are inside the oscillatory region.

3. region **AB**: trajectories of the full system may approach one of two different solutions in the (h_1, h_2) plane, depending if we start below or above the identity line. Presence of the averaged nullclines inside the oscillatory region intersecting at a single (unstable) fixed point near the identity line. Transition from **SB** and **AB** when averaged nullclines enter oscillatory region.

4. region $\tilde{\mathbf{BS}}$. System is bursting. As in figure 3(B) there are 2 fixed points in O. If we start with $h_2 < h_1$, then trajectories of the full system exit the boundary Ω. If $h_1 < h_2$, trajectories of the full system cross Ω at some point above the line $h_1 = h_2$ (figure not shown). Transition from **AB** to $\tilde{\mathbf{BS}}$ happens with an unstable fixed point entering O for $h_1 > h_2$ through Ω. There are other possibilities of transition which have to be further explored.

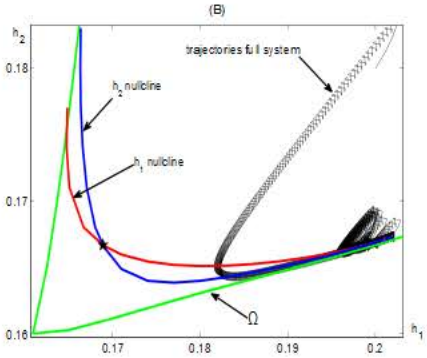

Figura 3: Solution on region $\tilde{\mathbf{BS}}$ with $g_{ton} = 0.84$, $g_{syn} = 3$ and $\delta = 0.01$. (B) Boundary of oscillatory region Ω with averaged nullclines h_1 and h_2 showing two fixed points in O, with trajectories of the full system plotted together.

5. region **BS**: There are 2 fixed points inside O and system is bursting or spiking depending on initial conditions. If one starts above $h_2 = h_1$, with $h_2 > h_1$, then trajectories of the full system (1)-(4) leave the oscillatory region above the identity line and system bursts. Otherwise, the system spikes. In figure 4, a plot is shown for a representative of this region displaying the boundary of the oscillatory region Ω and the averaged nullclines along with the locations of the two fixed points and the trajectories of the full system for different initial conditions. Note also in figure 4, the presence of a new region $\tilde{O}$. This region on the (h_1, h_2) parameter space correspond to pairs (h_1, h_2) for which the fast subsystem has B_p.

6. region $\mathbf{B}_0$: For $g_{syn} = 3$ and $\delta > 0.03$ system is bursting, for any initial condition. Our conjecture is that the averaged nullclines do not intersect inside the oscillatory region. In this region, for any initial condition trajectories of the full system leave O through Ω above the identity line. We believe that the transition from **BS** and $\mathbf{B}_0$ occurs through a saddle node bifurcation.

7. region **AS**: System is tonically spiking with three fixed points: two inside O and one in $\tilde{O}$ (figure 5(Left)). Starting above $h_1 = h_2$ line, then the system goes to upper fixed point, otherwise goes to the lower fixed point. For low values of δ, the transition from **BS** to **AS** will take place through C_{01} when a (stable) fixed point enters $\tilde{O}$. Transition from **AS** to $\mathbf{B}_0$ when upper fixed point exits at the cusp through $\tilde{O}$ and the other two fixed points are lost due to the saddle node (codimension 2 bifurcation).

ISSN 1984-8218

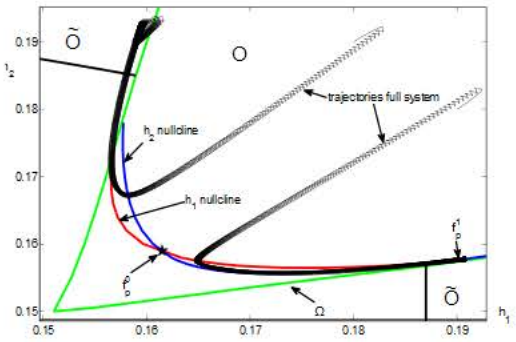

Figura 4: Solutions corresponding to region **BS** with $g_{ton} = 0.859$, $g_{syn} = 3$ and $\delta = 0.01$.

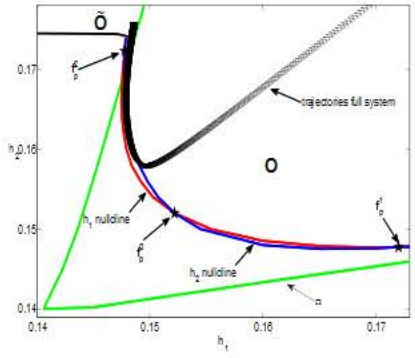

Figura 5: Left: Representative of region **AS** for $g_{ton} = 0.88$, $g_{syn} = 3$ and $\delta = 0.01$, along with the trajectories of the full system for initial conditions with $h_2 > h_1$. Right: Representative of region $\tilde{\mathbf{AS}}$ for $g_{ton} = 0.88$, $g_{syn} = 3$ and $\delta = 0.02$

8. region $\tilde{\mathbf{AS}}$: System is tonically spiking with one (stable) fixed point. Inside O the 2 nullclines are very close together for some values of h_1 and h_2 (figure 5(Right)). For some initial conditions the trajectories of the full system may hang around the two averaged nullclines for a while before it moves toward the fixed point. This transition from 3 fixed points to only 1 fixed point, i.e., from **AS** to $\tilde{\mathbf{AS}}$, can only occur if the system passes through a saddle node point. Therefore, the curve C_{SN} represents a curve of saddle node points for increasing δ. Finally, the transition from $\mathbf{B}_0$ to $\tilde{\mathbf{AS}}$ occurs due to a fixed point entering $\tilde{O}$ through C_{01}. Note that the fixed point f_p^2 in $\tilde{\mathbf{AS}}$ can, in theory, move to region O.

3.1.2 Different regions of bursting and spiking for $g_{syn} = 6, 9$

For $g_{syn} = 6$, different regions were characterized which are equivalent to the regions found in [3] (figure not shown). One important and expected difference of the region found in the heterogeneous case and the homogeneous case was the fact that the fixed point of the averaged nullclines did not take place on the identity line as it was happening before (not shown). Some numerical difficulties arose in order to determine precisely the location of each nullcline, although further computation showed us that these nullclines are reasonably positioned (not shown here).

For $g_{syn} = 9$, there was no significant difference fund from the transitions for the homogeneous case, for the level of heterogeneity applied.

ISSN 1984-8218

4 Conclusions

Many differences arose when comparing the homogeneous ($g_{NaP_1} = g_{NaP_2}$) and heterogeneous ($g_{NaP_1} \neq g_{NaP_2}$). First, for the heterogeneous case we could not make the same analysis for general values of g_{ton} and g_{syn} as Best *et al* [3] did in the homogeneous case. We had to compute boundaries of spiking and bursting for particular values of g_{syn} and different values of δ when varying g_{ton}.

For the homogeneous case, we have that for any given value of g_{syn} the boundary between quiescence and bursting had a value of g_{ton} that was almost the same for all values of g_{syn} (see [3]). For $\delta = 0.1$, the transition between quiescence and bursting takes place for some g_{ton} between 0.23 and 0.24. Therefore, the two cells in the heterogeneous case tend to become active for lower external inputs.

In theory, with increasing of heterogeneity we have chance to have bursting for a bigger interval of g_{ton}. That is, bursting should start with smaller external inputs applied to the system. This change in the boundary Q-**SB** was observed for $g_{syn} = 3$ and $g_{syn} = 6$.

For $g_{syn} = 3$, if we consider all the regions where the cell presents some type of bursting, the range of g_{ton} for which we have bursting is bigger than for the homogeneous case, although we have some dependency on initial conditions and one type of bursting is transitional. This shows that heterogeneity increases our chances of having a larger range of parameters where bursting is possible [5]. This wider range of bursting shows how heterogeneity can help adaptability for the respiratory system. Therefore, better understanding of this network using mathematical models can be of great help in understanding some of the diseases attacking our respiratory system.

Referências

[1] M. E. Alexianu, B.-K. Ho, A. H. Mohamed, V. La Bella, R. G. Smith, and S. H. Appel. The role of calcium-binding proteins in selective motoneuron vulnerability in amyotrophy lateral sclerosis. *Ann. Neuro.*, 36:846-858, 1994.

[2] E.E. Benarroch, A.M. Schmeichel, P.A. Low, and J.E. Parisi. Depletion of ven- tromedullary nk-1 receptor-immunoreactive neurons in multiple system atrophy. *Brain*, 126:2183-2190, 2003.

[3] J. Best, A. Borisyuk, J. Rubin, D. Terman, and M. Welschselberger. The dynamic range of bursting in a model respiratory pacemaker network. *SIAM J. Appl. Dyn. Syst.*, 4:1107-1139, 2005.

[4] R. Butera, J. Rinzel, and J. Smith. Models of respiratory rhythm generation in the pre-bötzinger complex. I. bursting pacemaker neurons. *J. Neurophysiol.*, 82:382-397, 1999.

[5] R. Butera, J. Rinzel, and J. Smith. Models of respiratory rhythm generation in the pre-bötzinger complex. II. population of coupled pacemaker. *J. Neurophysiol.*, 82:398-415, 1999.

[6] B. Ermentrout. Simulating, Analyzing, and Animating Dynamical Systems: A Guide to XPPAUT for Researchers and Students. *Software Environ. Tools 14, SIAM*, Philadelphia, 2002.

[7] J.L. Feldman and C.A. Del Negro. Looking for inspiration: new perspectives on respiratory rhythm. *Nature*, 7:232-242, 2006.

[8] A. L. Hodgkin and A. F. Huxley. A quantitative description of membrane current and its application to conduction and excitation in nerve. *J.Physiol.*(London), 4:500-544, 1952.

[9] J.C. Smith, H.H. Ellenberger, K. Ballayi, D.W. Richter, and J.L. Feldman. Pre-Bötzinger complex: A brainstem region that may generate respiratory rhythm in mammals. *Science*, 254:726-729, 1991.